



CHORUS

This is the accepted manuscript made available via CHORUS. The article has been published as:

Renormalization group for a continuous-time quantum search in finite dimensions

Shanshan Li and Stefan Boettcher

Phys. Rev. A **95**, 032301 — Published 2 March 2017

DOI: [10.1103/PhysRevA.95.032301](https://doi.org/10.1103/PhysRevA.95.032301)

Renormalization Group for Continuous Time Quantum Search in finite Dimensions

Shanshan Li and Stefan Boettcher

Department of Physics, Emory University, Atlanta, GA 30322; USA

We consider the quantum search problem with a continuous time quantum walk for networks characterized by a finite spectral dimension d_s of the network Laplacian. For general networks of fractal (integer or non-integer) dimension d_f , for which in general $d_f \neq d_s$, it suggests that it is d_s that determines the computational complexity of the quantum search. Our results continue those of Childs and Goldstone for lattices of integer dimension, where $d = d_f = d_s$. Thus, we find for general fractals that the Grover limit of quantum search can be obtained whenever $d_s > 4$. This complements the recent discussion of mean-field (i.e., $d_s \rightarrow \infty$) networks by Chakraborty et al. showing that for all those networks spatial search by quantum walk is optimal.

PACS numbers: 05.10.Cc, 03.67.Ac, 05.40.Fb

I. INTRODUCTION

Quantum search present one of the frameworks for which quantum computing can satisfy its promise to provide a significant speed-up over classical computation. Grover [1] has shown that search based on a quantum walk can locate an entry in an unordered list of N sites in a time that scales as $\sim \sqrt{N}$, a quadratic speed-up over classical search algorithms. However, that finding was based on a list in which all sites are interconnected with each other, thus, raising the question regarding the impact of geometry on this result. Note, for instance, that if the walk had to pass information through the list over a linear, $1d$ -line of sites, no quantum effect would provide an advantage over simply passing every site until the desired entry is located. In fact, Childs and Goldstone [2] have discussed an elementary quantum search and found that it can reach the Grover limit only on lattices in dimensions $d > 4$. Aaronson and Ambainis [3] proposed an extended quantum search algorithm that finds a marked entry in time of order $\sim \sqrt{N}$ for lattices with $d > 2$, and in time $\sim \sqrt{N} \log^2 N$ for $d = 2$, using recursive search on sub-cubes. Similarly, modified quantum walk algorithms exist, such as with a “coined” discrete-time quantum walk, that do achieve Grover efficiency down to $d = 2$ (up to logarithmic corrections), but require additional internal degrees of freedom [4]. Even beyond search, understanding what controls the behavior of quantum walks remains a desirable goal. For instance, it presents a natural framework that serves as a universal computational primitive for quantum computation [5].

Here, we explore which aspect of the underlying geometry has the most significant impact by considering a basic quantum search without extra features and find that then it is the spectral dimension d_s of the network which controls the algorithmic complexity. Following Ref. [2], we consider here the continuous time quantum walk (CTQW) that can be defined in any geometry by the Hamiltonian

$$\mathcal{H} = \gamma \mathbf{L} - |w\rangle \langle w|, \quad (1)$$

where \mathbf{L} is the Laplacian matrix, and $|w\rangle \langle w|$ is the projection operator (the oracle) for some target site w . With that, a quadratic speedup for quantum search has been shown for high dimensional graphs such as the complete graph [6] and the hypercube [7, 8]. Recently, it has been proven also to be optimal on Erdős-Rényi graphs with N sites as long as the existence probability for an edge between any two sites is $p \gtrsim \log^{3/2} N/N$ or the graphs are regular, i.e., they have the same degree for every site [9]. For finite dimensional lattices, it was shown [2] that the quantum search in Eq. (1) can reach the Grover limit on lattices in dimensions $d > 4$ only, while in $d = 4$, the running time to achieve a success probability of order 1 is $\sim \sqrt{N} \log^{3/2} N$, with increasing deviations from \sqrt{N} -scaling for $d = 3$ and 2. In contrast, a discrete-time, coined version of a quantum walk has been proposed by which quantum search falls short of the Grover limit in $d = 2$ only by logarithmic factors [4, 10]. Similarly, using an appropriate lattices version of a Dirac Hamiltonian possessing extra spin degrees of freedom, Childs and Goldstone [11] proposed a CTQW that competes with the discrete time case with a time of order $\sim \sqrt{N}$ for $d > 2$ and of order $\sim \sqrt{N} \log N$ for $d = 2$. The additional spin space introduces a linear dispersion relation near the Dirac point. Foulger et al [12] exploited the Dirac point of the walk Hamiltonian on a graphene lattice to find the marked entry in time $\sim \sqrt{N} \log^{3/2} N$ for $d = 2$ without using extra space. Childs [13] further generalized the idea of a Dirac point by considering CTQW on crystal lattices, where the Hamiltonian is constructed without external memory by embedding these additional degrees of freedom into the lattice as extra vertices.

While previous studies focus on CTQW in translationally invariant lattices, here, we continue to generic structures with arbitrary real (fractal) dimensions $d = d_f$ by studying the Hamiltonian defined in Eq. (1) on fractals. We aim to understand how geometrical parameters affect the dynamics of the CTQW. Fractals generally possess both a fractal dimension d_f and a spectral dimension d_s that can vary independently to characterize their geometry [14–16], while for regular lattices $d_f = d_s = d$. In the context of a network Laplacian (or, equivalently, its adjacency matrix), the fractal dimension d_f is best obtained as the number of distinct vertices (“volume” V) that can be reached, on average over all initial vertices, within r jumps, i.e., $\langle V(r) \rangle \sim r^{d_f}$ for large r . In turn, the spectral dimension d_s is more subtle as it refers to the scaling with system size N of the lowest (non-zero) eigenvalues, $\lambda_i \sim N^{-2/d_s}$, in the Laplacian spectrum. Since many physical properties of a system, such as elastic response or transport via the wave or the diffusion equation, are intimately linked to the Laplacian, their dispersion relations are significantly impacted by these dimensions. For example, in the absence of further interaction potentials, free diffusion on any fractal is then characterized simply in terms of the random walk dimension $d_w = 2d_f/d_s$. Using scaling as well as exact renormalization group (RG) arguments, which we have developed recently [17], we show in the following that the spectral dimension d_s of the lattice Laplacian controls the ability of CTQW to saturate the Grover limit generally. This result becomes most significant for non-integer dimensions, especially when $d_f \neq d_s$.

Graphs with fractal dimensions have been considered previously for search with CTQW [18]. The fractals chosen there include dual Sierpinski gaskets, T-fractals, Cayley trees, and Cartesian products between Euclidean lattices and dual Sierpinski gaskets, with a variety of fractal and spectral dimensions. Based on numerical simulations, it was suggested that whether CTQW provides quadratic speedup is determined together by a spectral dimension larger

than 4 and by the overlaps of the initial state with the ground and first excited state of the Hamiltonian. These overlaps undergo a critical transition near the closest “gap” between both levels, controlled by the choice of γ in Eq. (1). We explicitly relate the transition in γ to (derivatives of) the Laplacian determinant using a spectral ζ -function. Using exact RG developed in Ref. [19], we have shown recently [17] that the asymptotic scaling of the Laplacian determinant is described uniquely in terms of d_s .

The paper is organized as follows: In Sec. II, we review the formulation of the widely-studied continuous-time quantum search algorithm, while in Sec. III we focus on that aspect of the algorithm which refers to the Laplacian spectrum to apply the general result obtained in Ref. [17]. In Sec. IV, we apply this result to determine the computational complexity of our quantum search for non-integer dimensions. We conclude with Sec. V. The technical details required to appreciate the renormalization group arguments that lead to the main result of Sec. III are recalled in the Appendix.

II. A CONTINUOUS-TIME QUANTUM SEARCH

The continuous time quantum walk on a graph is determined by the Schrödinger equation evolving in a Hilbert space spanned by the N -position site-basis $|x\rangle$,

$$i \frac{d\Psi_x(t)}{dt} = \sum_y \mathcal{H}_{xy} \Psi_x(t), \quad (2)$$

where $\Psi_x(t) = \langle x | \Psi(t) \rangle$ is the complex amplitude at site x , and \mathcal{H} is the Hamiltonian defined in Eq. (1). The search typically evolves from an initial state that is prepared as the uniform superposition over all sites [1], $|s\rangle = \frac{1}{\sqrt{N}} \sum_x |x\rangle$.

The complete graph is a special case of CTQW, where it suffices to consider the subspace spanned by $|s\rangle$ and $|w\rangle$ on which the Hamiltonian acts nontrivially. At $\gamma N = 1$, the ground and first excited state are respectively $(|w\rangle \pm |s\rangle) / \sqrt{2}$ with a energy gap of $2/\sqrt{N}$. The search Hamiltonian achieves success by driving the system from state $|s\rangle$ to $|w\rangle$ with a transition probability $\Pi_{s,w} = |\langle w | e^{-i\mathcal{H}t} | s \rangle|^2 = \sin^2\left(t/\sqrt{N}\right)$ that reaches unity first at time $t = \frac{\pi}{2}\sqrt{N}$. For a general geometry, the ground and first excited state are more complicate than a superposition of $|s\rangle$ and $|w\rangle$. Yet, the objective of CTQW remains two-fold: (1) find a critical value $\gamma = \gamma_c$ such that the overlaps between $|s\rangle$ as well as $|w\rangle$ and the ground and first excited state are substantial, and (2) ascertain that at this critical point the Hamiltonian drives a transition from $|s\rangle$ to $|w\rangle$ in a time $t \sim 1/(E_1 - E_0) \sim \sqrt{N}$.

We denote eigenvalues and normalized orthogonal eigenstates for \mathcal{H} and \mathbf{L} respectively as $\{E_i, |\psi_i\rangle\}$ and $\{\lambda_i, |\phi_i\rangle\}$ for $0 \leq i < N$. Note that the initial state $|s\rangle = |\phi_0\rangle$ is, in fact, the lowest eigenstate of the Laplacian with $\mathbf{L}|s\rangle = 0$, i.e., the associated eigenvalue is $\lambda_0 = 0$, while all other Laplacian eigenvalues are positive. Ref. [2] has derived a spectral function for \mathcal{H} in terms of the Laplacian eigenstates that is convenient for the discussion of translationally invariant lattices:

$$F(E) = \left\langle w \left| \frac{1}{\gamma \mathbf{L} - E} \right| w \right\rangle = \sum_{i=0}^{N-1} \frac{|\langle w | \phi_i \rangle|^2}{\gamma \lambda_i - E}. \quad (3)$$

The condition on the Hamiltonian eigenvalues,

$$F(E_i) = 1, \quad (4)$$

is provided in terms of the Laplacian eigenvalues. From the spectral function, one can derive the overlap of any eigenstate with the initial state as

$$|\langle s | \psi_i \rangle|^2 = \frac{1}{N E_i^2 F'(E_i)}. \quad (5)$$

The key objective of a quantum search concerns optimizing the transition amplitude between the initial state and the target site,

$$\langle w | e^{i\mathcal{H}t} | s \rangle = -\frac{1}{\sqrt{N}} \sum_{i=0}^{N-1} \frac{e^{iE_i t}}{E_i F'(E_i)}. \quad (6)$$

The Hamiltonian \mathcal{H} (i.e., γ) has to be optimized such that this amplitude reaches a finite magnitude in the shortest amount of time in the limit of large N .

III. QUANTUM SEARCH ON FRACTAL NETWORKS

For regular lattices, the overlap of the eigenstates of the Laplacian with any member of the site basis, in particular $|w\rangle$, is uniform and *independent* of w . However, this is generally not true for fractals [15]; such heterogeneity could lead to a large variability in the “findability” of a significant number of ill-placed sites w [20]. For our purposes here, we have to assume that for typical sites w of the fractal networks, the overlaps with eigenvectors of the Laplacian still satisfy

$$|\langle w|\phi_i\rangle|^2 \sim \frac{1}{N}, \quad (7)$$

to remove this factor in the sum of Eq. (3), as can be done for the Fourier modes of the regular lattice of integer d . In fact, for the networks considered here, the Migdal-Kadanoff renormalization group (MKRG) of hyper-cubic lattices described in Appendix A, we will show numerically in Sec. IV A that Eq. (7) holds for typical sites. While we can only assert the relation in Eq. (7) numerically, any violation would merely be an artifact of the heterogeneity introduced by the MKRG, and it should be reassuring that the relation appears to be satisfied for the most generic sites of the network.

With that, and using $\lambda_0 = 0$, Eq. (3) can be rewritten as

$$F(E) \sim -\frac{1}{NE} + \frac{1}{\gamma} I_1 + \frac{1}{N} \sum_{i=1}^{N-1} \frac{E}{\gamma\lambda_i(\gamma\lambda_i - E)}, \quad (8)$$

defining the spectral ζ -function [21, 22]

$$I_j \sim \frac{1}{N} \sum_{i=1}^{N-1} \left(\frac{1}{\lambda_i}\right)^j, \quad (9)$$

which plays a central role in the analysis. These quantities have been considered before, in particular by Ref. [2], to examine search by CTQW on regular lattices, or in Ref. [18] for fractals. In Ref. [18], it was assumed that Eq. (9) requires complete knowledge of the entire Laplacian spectrum, which is rarely achievable. Here, we want to point out that I_j can be reduced to the evaluation of the determinant of \mathbf{L} and derivatives thereof. Identifying

$$\begin{aligned} \sum_{i=1}^{N-1} \ln \lambda_i &= \ln \left[\frac{1}{\epsilon} \prod_{i=0}^{N-1} (\lambda_i + \epsilon) \right]_{\epsilon \rightarrow 0}, \\ &= \ln \left[\frac{1}{\epsilon} \det(\mathbf{L} + \epsilon \mathbf{1}) \right]_{\epsilon \rightarrow 0}, \end{aligned}$$

we have obtained in Ref. [17] (see also Appendix B) the asymptotic behavior of the spectral ζ -function defined in Eq. (9) as

$$I_j \sim \left(\frac{\partial}{\partial \epsilon} \right)^j \ln \left[\frac{1}{\epsilon} \det(\mathbf{L} + \epsilon \mathbf{1}) \right] \Big|_{\epsilon \rightarrow 0} \quad (10)$$

$$\sim \begin{cases} N^{\frac{2j}{d_s}-1}, & d_s < 2j, \\ \text{const}, & d_s > 2j, \end{cases} \quad (11)$$

for fractal networks with the spectral dimension d_s . Thus, d_s becomes the key characteristic for any network, such as those fractals for which $d = d_f \neq d_s$, that determines whether the Grover limit can be achieved. For example, as observed in Ref. [2], this quantum search becomes optimal for lattices of any dimension when there is a phase transition in the overlaps $|\langle s|\psi_0\rangle|^2$ and $|\langle s|\psi_1\rangle|^2$, of which the former rises while the latter declines for increasing γ . This critical point occurs for

$$\gamma \sim \gamma_c = I_1. \quad (12)$$

Accordingly, we find for general fractal networks that

$$\gamma_c \sim \begin{cases} N^{\frac{2}{d_s}-1}, & d_s < 2, \\ \text{const}, & d_s > 2. \end{cases} \quad (13)$$

IV. COMPLEXITY OF QUANTUM SEARCH IN NON-INTEGER DIMENSIONS

To obtain the runtime complexity for the quantum search, we have to distinguish the following cases: For $d_s > 4$, according to Eq. (10), both $I_{1,2}$ remain constant. It is then self-consistent to consider the spectral function in Eq. (8) for energies $|E| \ll \gamma_c \lambda_1$, which applies to both the ground state E_0 and the first excited state E_1 of \mathcal{H} near the optimal (“critical”) γ_c . Expanding the remaining sum in Eq. (8) to leading order in E yields

$$F(E) \sim -\frac{1}{NE} + \frac{1}{\gamma} I_1 + \frac{E}{\gamma^2} I_2 + \dots, \quad (|E| \ll \gamma_c \lambda_1), \quad (14)$$

Since $F(E_{0,1}) = 1$ from the eigenvalue condition in Eq. (4), we obtain a consistent balance to leading and sub-leading order only for $\gamma = \gamma_c = I_1$, thereby validating Eq. (12), and for $\frac{1}{NE_{0,1}} \sim \frac{E_{0,1}}{\gamma^2} I_2 \ll 1$, yielding

$$E_{0,1} \sim \pm \frac{1}{\sqrt{N}} \frac{I_1}{\sqrt{I_2}} = O\left(N^{-\frac{1}{2}}\right). \quad (15)$$

Then, the derivative of Eq. (14) provides $F'(E_{0,1}) \sim 2I_2/I_1^2$ such that according to Eq. (5) the initial state $|s\rangle$ overlaps with equal and finite weight with both, ground state and first excited state:

$$|\langle s | \psi_{0,1} \rangle|^2 \sim \frac{1}{2}. \quad (16)$$

As $E_i > \gamma_c \lambda_1$ for all $i \geq 2$, higher energy eigenstates do not contribute for large N , and we obtain from the first two terms of the transition amplitude in Eq. (6),

$$|\langle w | e^{i\mathcal{H}t} | s \rangle|^2 \sim \frac{1}{N} \left| \frac{e^{iE_0 t}}{E_0 F'(E_0)} + \frac{e^{iE_1 t}}{E_1 F'(E_1)} \right|^2, \quad (17)$$

$$\sim \frac{I_1^2}{I_2} \sin^2 \left(\frac{2I_1}{\sqrt{I_2}} \frac{t}{\sqrt{N}} \right). \quad (18)$$

Thus, the transition probability oscillates and reaches its first maximum at a time

$$t = t_{\text{opt}} \sim \frac{\sqrt{I_2}}{I_1} \sqrt{N} = O\left(N^{\frac{1}{2}}\right), \quad (19)$$

at which point the transition probability becomes

$$p_{\text{opt}} = |\langle w | e^{i\mathcal{H}t_{\text{opt}}} | s \rangle|^2 \sim \frac{I_1^2}{I_2} = O(1). \quad (20)$$

Finally, to find the targeted site w with a probability of order unity, we need to run the quantum search $\sim 1/p_{\text{opt}}$ times, each for a time of t_{opt} at which a measurement must be executed. Thus, the runtime complexity for a successful search is given by

$$\frac{t_{\text{opt}}}{p_{\text{opt}}} \sim \left(\frac{I_2}{I_1^2} \right)^{\frac{3}{2}} \sqrt{N} = O\left(N^{\frac{1}{2}}\right), \quad (d_s > 4). \quad (21)$$

For case $d_s = 4$, I_1 remains constant while $I_2 \sim \ln N$ acquires a logarithmic correction in the limit $d_s \rightarrow 4$. With that, the analysis of the previous case remains applicable, although the condition $|E| \ll \gamma_c \lambda_1$ is merely logarithmically satisfied. Thus, we obtain from Eq. (21) in this interpretation that

$$\frac{t_{\text{opt}}}{p_{\text{opt}}} = O\left(N^{\frac{1}{2}} \ln^{\frac{3}{2}} N\right), \quad (d_s = 4). \quad (22)$$

For case $2 < d_s < 4$, I_1 remains constant while $I_2 \sim N^{\frac{4}{d_s}-1}$. However, by Eq. (15), this would imply $E_{0,1} \sim N^{-\frac{2}{d_s}}$, which would violate the condition of $E_{0,1} \ll \gamma_c \lambda_1$ where $\lambda_1 \sim \Lambda N^{-\frac{2}{d_s}}$. As a consequence, the expansion in Eq. (14) is no longer valid and we have to reconsider Eq. (8) anew at $\gamma = \gamma_c \sim I_1$, but with $\gamma_c \lambda_1 \sim E_{0,1} = e_{0,1} I_1 \Lambda N^{-\frac{2}{d_s}}$. Then, Eq. (8) provides

$$F(E_{0,1}) \sim 1 - \frac{1}{I_1 \Lambda e_{0,1}} N^{\frac{2}{d_s}-1} + \frac{e_{0,1}}{I_1 \Lambda (1 - e_{0,1})} N^{\frac{2}{d_s}-1} + \dots, \quad (23)$$

where the two leading corrections cancel self-consistently with a negative (positive) solution for e_0 (e_1). Then, $E_{0,1}F'(E_{0,1}) \sim N^{\frac{2}{d_s}-1}$, such that by Eq. (18), the transition probability diminishes for falling d_s and is at best

$$|\langle w | e^{i\mathcal{H}t} | s \rangle|^2 \lesssim \frac{1}{N} \left| \frac{1}{E_0 F'(E_0)} \right|^2 \sim N^{1-\frac{4}{d_s}}. \quad (24)$$

In turn, to accomplish any significant change in this transition amplitude requires at time of at least $t_{opt} \gtrsim |\langle w | e^{i\mathcal{H}t} | s \rangle| \sqrt{N} \sim N^{1-\frac{2}{d_s}}$. Thus, the runtime complexity finally is asymptotically bounded by

$$\frac{t_{opt}}{p_{opt}} \gtrsim N^{\frac{2}{d_s}}, \quad (2 < d_s < 4). \quad (25)$$

which for $d_s \rightarrow 2$ also reproduces the known conclusion for the $2d$ regular lattice, up to logarithmic corrections.

A. Uniformity of the Overlap

Finally, we confirm numerically the assumption in Eq. (7) that for typical vertices w , the overlap with Laplacian eigenvectors scales as $|\langle w | \phi_i \rangle|^2 \sim 1/N$. For example, in Ref. [17], we have considered the Laplacians for fractal networks in the Migdal-Kadanoff renormalization group (MKRG) [24, 25], which mimic the properties of regular lattices quite closely and have $d_s = d_f = d$ but can take one such values also for non-integer dimensions, as described in Fig. 2. Unlike for regular lattices, though, in MKRG sites are arranged in a hierarchical network [26] in which at each level of the hierarchy the system size expands by a factor of $\sim 2^{d-1}$. Those newly added sites all are locally equivalent, but they are distinct from previous levels, making the network more heterogeneous than the lattice it is meant to represent. However, since they constitute by far the largest fraction and are the most uniform, sites in the highest level of the hierarchy exhibit what can be considered as the typical behavior. In Fig. 1, we have plotted the overlaps for searched-for sites w with all eigenvectors $|\phi_i\rangle$, $0 \leq i < N$ of the respective Laplacian but averaged separately over all w in the highest, 2nd-highest, and 3rd-highest levels of the hierarchy for MKRG networks of $b = 2$ after $g = 6$ generations of the hierarchy, and for $b = 3$ after $g = 5$ generation. For sites w in the highest level, the overlaps are essentially uniform and satisfy Eq. (7) for all i . For w on lower levels, their overlaps with an increasing number of eigenvectors related to the largest eigenvalues λ_i outright vanishes, while the non-vanishing overlaps remain with few exceptions uniform and $O(1/N)$. This fact suggests that the runtime complexity differs mildly between sites w in different hierarchies. For our purpose here, we conclude that sites w in the highest level are most representative of the behavior of any site on a regular lattice.

V. CONCLUSIONS

In conclusion, we have studied search by a continuous-time quantum walk on fractal networks and, by reference to properties of spectral ζ -functions [17], identified the dominant role of the spectral dimension d_s in controlling the search efficiency and in setting the condition for attaining the Grover limit, for $d_s > 4$. Particularly, we reproduce the known results in regular lattices with integer $d = d_s$ and generalize them to hyper-cubic lattices in arbitrary lattice dimensions d using the Migdal-Kadanoff renormalization group. Although this family of fractals is chosen to satisfy $d_s = d_f = d$, the analysis in Ref. [17] that leads to Eq. (10) implies the preeminence of d_s also for search on other fractals, as had been suggested previously in numerical studies [18].

Acknowledgements: We acknowledge financial support from the U. S. National Science Foundation through grant DMR-1207431.

APPENDIX

A. Migdal-Kadanoff renormalization group

The Migdal-Kadanoff renormalization group (MKRG) [24–26] is a bond-moving scheme that approximates d -dimensional lattices. It often provides excellent approximations for $d = 2$ and 3 [27], and it becomes trivially exact in $d = 1$. The networks resulting from MKRG have a simple recursive, yet geometric, structure and have been widely studied in statistical physics [28–30]. Starting from generation μ with a single bond, at each subsequent generation $\mu + 1$, all bonds are replaced with a new sub-graph. This structure of the sub-graph arises from the bond-moving

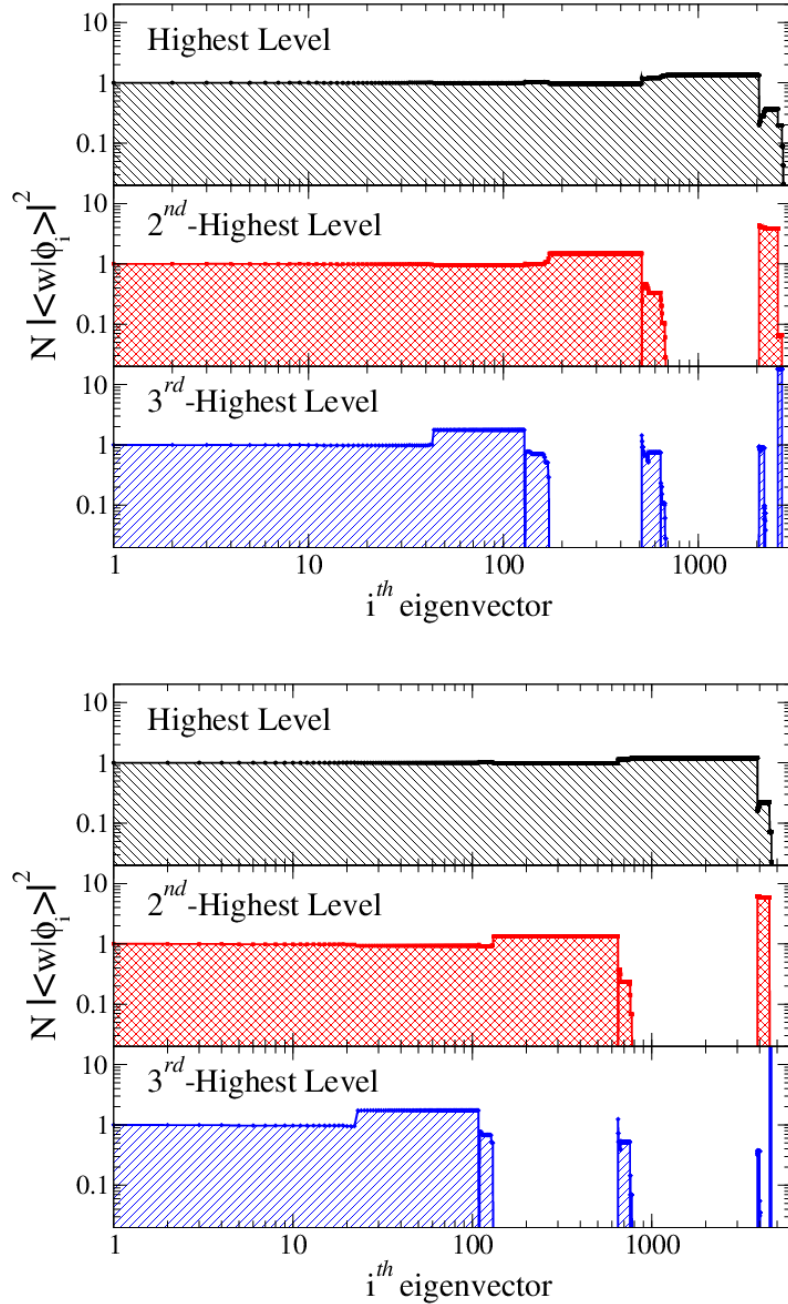


Figure 1. Plot of the overlaps $|\langle w|\phi_i\rangle|^2$ in MKRG for the searched-for sites w with the Laplacian eigenvectors ϕ_i as a function of i , ordered such that respective eigenvalues satisfy $\lambda_i \leq \lambda_{i'}$ for any two indices $i \leq i'$. The MKRG used here [23] rescales length by $l = 2$ with (a) $b = 2$ and (b) $b = 3$ branches in each RG-step for an effective dimension $d = 1 + \log_l b$ of (a) $d = 2$ and (b) $d = 2.585\dots$. The RG has been iterated for $g = 6$ generations in the hierarchy in (a), forming a lattice of $N = 2 + \frac{b}{2b-1} [(2b)^g - 1] = 2732$ sites, and in (b) for $g = 5$ with $N = 4667$ sites. In the top panel of both, (a) and (b), the overlaps (rescaled by a factor of N) were averaged over all sites w in the highest hierarchical level g , in the middle panel overlaps were averaged only over those w in level $g - 1$, and in the respective bottom panel for level $g - 2$. Note that every level the number of sites increases by a factor of $\sim 2b$, such that the vast majority of all sites w are typically located in these highest levels of the hierarchy. For those, these plots show that indeed $N|\langle w|\phi_i\rangle|^2 \sim 1$, typically, as assumed in Eq. (7), although these overlaps progressively vanish for those w in lower levels for eigenvectors of larger index i .

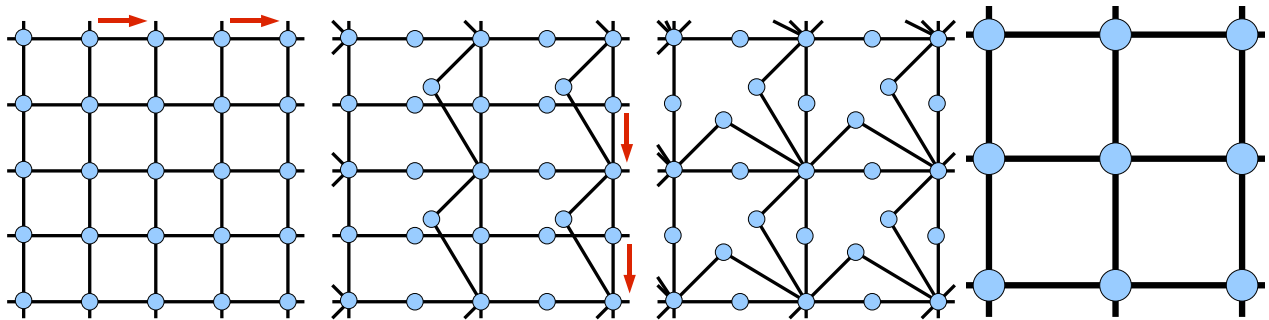


Figure 2. Bond-moving scheme in the Migdal–Kadanoff renormalization group, here for a square lattice ($d = 2$) with $l = 2$, i. e. $b = 2$ in Eq. (26). Starting from the lattice with unit bonds (a), bonds in intervening hyper-planes are projected onto every l^{th} plane in one direction while bonds connect to the l^{th} plane only at every l^{th} vertex (b), which is then repeated in subsequent directions (c), to re-obtain a similar hyper-cubic lattice, now of bond-length l (d). The renormalized bonds in this case consist of $b = l^{d-1} = 2$ branches, each of a series of $l = 2$ bonds; the general RG-step for $l = 2$ and arbitrary branches b is depicted in Fig. 3

scheme in d dimensions [24, 25], as depicted in Fig. 2: In a hyper-cubic lattice of unit bond length, at first all $l - 1$ intervening hyper-planes of bonds, transverse to a chosen direction, are projected into every l^{th} hyper-plane, followed by the same step for $l - 1$ hyper-planes being projected onto the l^{th} plane in the next direction, and so on. In the end, as shown in Fig. 3, one obtains a renormalized hyper-cubic lattice (of bond length l) in generation $\mu + 1$ with a renormalized bond of generation $\mu + 1$ consisting of a sub-graph of

$$b = l^{d-1} \quad (26)$$

parallel branches, each having of a series of l bonds of generation μ . In turn, we can rewrite Eq. (26) as

$$d = 1 + \log_l b, \quad (27)$$

anticipating analytic continuation in l and b to obtain results for arbitrary, *real* dimensions d . In the following, we consider a general series of Migdal-Kadanoff networks by varying b while fixing $l = 2$.

B. RG for the Spectral Determinant of Migdal-Kadanoff

The determinant of $\mathcal{L}(\epsilon) = \mathbf{L} + \epsilon \mathbf{1}$ in Eq. (10) for fractal lattices can be evaluated asymptotically in a recursive renormalization scheme. We have already described the procedure in great detail in Ref. [19]. In general, we employ the well-known formal identity [31],

$$\frac{1}{\sqrt{\det \mathcal{L}}} = \int \cdots \int_{-\infty}^{\infty} \left(\prod_{i=1}^N \frac{dx_i}{\sqrt{\pi}} \right) \exp \left\{ - \sum_{n=1}^N \sum_{m=1}^N x_n \mathcal{L}_{n,m} x_m \right\}. \quad (28)$$

For the RG, we employ a hierarchical scheme by which at each step μ a fraction $1/b$ of all remaining variables get integrated out while leaving the integral in Eq. (28) invariant, but now with $N' \leq N/b$ variables. Formally, say, in case of $b = 2$ we integrate out every odd-indexed variable in a network at step μ , we separate $\prod_{i=1}^N dx_i = \prod_{i=1}^{N/2} dx_{2i} \prod_{j=1}^{N/2} dx_{2j+1}$ and integrate to receive

$$\frac{1}{\sqrt{\det \mathcal{L}}} = C' \int \cdots \int_{-\infty}^{\infty} \left(\prod_{i=1}^{\frac{N}{2}} \frac{dx_{2i}}{\sqrt{\pi}} \right) \exp \left\{ - \sum_{n=1}^{\frac{N}{2}} \sum_{m=1}^{\frac{N}{2}} x_{2n} \mathcal{L}'_{n,m} x_{2m} \right\}, \quad (29)$$

where the reduced Laplacian \mathcal{L}' is now a $\frac{N}{2} \times \frac{N}{2}$ matrix that is formally *identical* with \mathcal{L} and C' is an overall scale-factor. That is, if $\mathcal{L} = \mathcal{L}(q, p, \dots)$ depends on some parameters, then $\mathcal{L}' = \mathcal{L}'(q', p', \dots)$ depends on those parameters in the same functional form, thereby revealing the RG-recursion relations, $q' = q'(q, p, \dots)$, $p' = p'(q, p, \dots)$, etc, and $C' = C'(q, p, \dots)$, that encapsulate all information of the original Laplacian. After a sufficient number of such

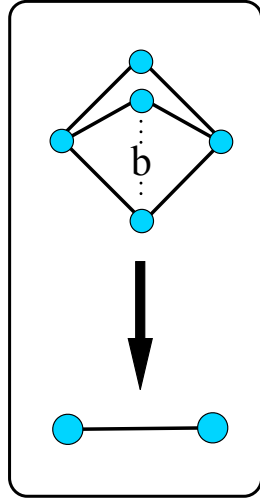


Figure 3. Hierarchical RG that results from the bond-moving scheme of any d -dimensional lattice shown in Fig. 2. A collection of b strings of l bonds at generation μ each ($l = 2$ here) gets renormalized into a single new bond at generation $\mu + 1$.

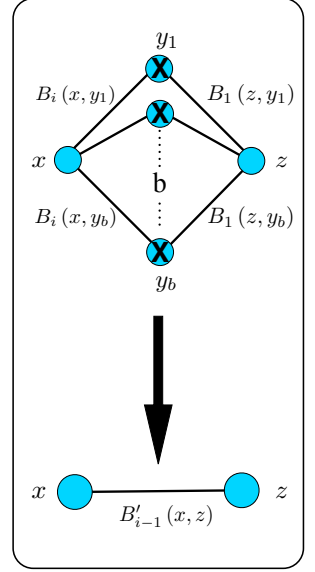


Figure 4. Graph-let for the MKRG for the spectral zeta-function, as adapted from the generic structure shown in Fig. 3. In that graph-let, the b inner vertices y_1, \dots, y_b belong to the currently lowest level ($i = 0$) of the hierarchy that will be integrated out (\times -mark) in the next RG-step. One of the two outer vertices, z , must be exactly one level higher ($i = 1$, here shown right). The other outer vertex, x , must be of some unspecified but higher level ($i > 1$, left). After the RG-step, symbolized by the arrow, the renormalized link B'_{i-1} is bound to have a vertex z with $i = 0$ on one end and some vertex x with $i' = i - 1 > 0$ on the other. A set of $2b$ of these links then become the input of the – identical – next RG-step.

RG-steps, a reduced Laplacian of merely a few variables remains that can be solved by elementary means. This property, of course, is very special and can be iterated in exact form only for certain types of fractal networks.

We can reconstruct the integral in Eq. (28) piece-by-piece by defining a simple algebra. As suggested by Fig. 2(c), in each RG-step the lattice consists of a collection of graph-lets of the type shown in Fig. 3, which we have adapted for the following calculation in Fig. 4. In that graph-let, the b inner vertices belong to the currently lowest level ($i = 0$) of the hierarchy that will be integrated out in the next RG-step. One of the two outer vertices is exactly one level higher ($i = 1$) as it would be integrated at the next step. The other outer vertex must be of some unspecified but higher level ($i > 1$). We can now define a helpful function pertaining to each bond, each of which is bound to have a vertex with $i = 0$ on one end and some vertex with $i > 0$ on the other. Its part of the integrand in Eq. (28) has the form

$$B_i(x, y) = C_i \exp \left\{ -\frac{q_i}{2} x^2 - \frac{q_0}{2} y^2 + 2pxy \right\}, \quad (30)$$

such that the RG-step depicted in Fig. 2(d) amounts to

$$\begin{aligned} B'_{i-1}(x, z) &= \int \cdots \int_{-\infty}^{\infty} \prod_{j=1}^b \frac{dy_j}{\sqrt{\pi}} B_i(x, y_j) B_1(z, y_j), \\ &= C_i^b C_1^b \exp \left\{ -\frac{b}{2} (q_i x^2 + q_1 z^2) \right\} \int \cdots \int_{-\infty}^{\infty} \prod_{j=1}^b \frac{dy_j}{\sqrt{\pi}} \exp \{ -q_0 y_j^2 + 2p(x+z)y_j \}, \\ &= C_i^b C_1^b q_0^{-\frac{b}{2}} \exp \left\{ -\frac{b}{2} \left(q_i - \frac{2p^2}{q_0} \right) x^2 - \frac{b}{2} \left(q_1 - \frac{2p^2}{q_0} \right) z^2 + 2b \frac{p^2}{q_0} xz \right\}, \\ &= C'_{i-1} \exp \left\{ -\frac{q'_{i-1}}{2} x^2 - \frac{q'_0}{2} z^2 + 2p'xz \right\}, \end{aligned} \quad (31)$$

where unprimed parameters are μ -times previously renormalized while primes indicate newly $\mu + 1$ -times renormalized parameters. From the last two lines, we can read off the RG-recursions at the μ^{th} step:

$$\begin{aligned} C_{i-1}^{(\mu+1)} &= \left(\frac{C_1^{(\mu)} C_i^{(\mu)}}{\sqrt{q_0^{(\mu)}}} \right)^b, \\ q_{i-1}^{(\mu+1)} &= b \left(q_i^{(\mu)} - \frac{2(p^{(\mu)})^2}{q_0^{(\mu)}} \right), \\ p^{(\mu+1)} &= b \frac{(p^{(\mu)})^2}{q_0^{(\mu)}}, \end{aligned} \quad (32)$$

for $i > 0$. Considering that initially, at $\mu = 0$ in the unrenormalized network, all vertex-weights defined in Eq. (30) are the same, $q_i^{(0)} \equiv 2$ for all i , the distinction between levels i in Eq. (32) disappears. Note that a vertex at level $i > 0$ contributes to the Gaussian integral $2b^i$ -fold through respective factors B_i , and 2-fold for $i = 0$ by appearing in two such factors $B_{i'}$, $i' > 0$. In this manner, the lattice Laplacian at $\mu = 0$ in Eq. (28) receives its proper weights on its diagonal. Equally, $C_i^{(0)} = 1$ for all $i > 0$. Thus, defining $C_\mu = C_i^{(\mu)}$, $p_\mu = b^{-\mu} p^{(\mu)}$, and $q_\mu = b^{-\mu} q_i^{(\mu)}$ for all $i \geq 0$, we obtain:

$$\begin{aligned} C_{\mu+1} &= \left[\frac{C_\mu^2}{\sqrt{b^\mu q_\mu}} \right]^b, \quad (C_0 = 1), \\ q_{\mu+1} &= q_\mu - 2 \frac{p_\mu^2}{q_\mu}, \quad (q_0 = 2 - \epsilon), \\ p_{\mu+1} &= \frac{p_\mu^2}{q_\mu}, \quad (p_0 = 1). \end{aligned} \quad (33)$$

Note that the recursions in Eq. (33) is not exactly identical to Eq. (32). With eigenvalue $\lambda = \epsilon$, the initial condition for $q_i^{(0)}$ Eq. (32) is, in fact,

$$\begin{aligned} q_i^{(0)} &= 2 - \epsilon/b^i, \quad 0 \leq i < k, \\ q_k^{(0)} &= 2 - 2\epsilon/b^k, \quad i = k, \end{aligned} \quad (34)$$

which does not allow to collapse the i -th hierarchy like in the Hanoi networks. However, in the Taylor expansion in small ϵ , order-by-order such a collapse is allowed. The difference between the $\{q_0^{(\mu)}, p^{(\mu)}\}$ from Eq. (33) and $\{q_\mu, p_\mu\}$ from Eq. (32) is

$$q_0^{(\mu)} - q_\mu \sim Q_1 \epsilon + Q_2 \epsilon^2 + Q_3 \epsilon^3 + \dots, \quad (35)$$

$$p^{(\mu)} - p_\mu \sim P_1 \epsilon + P_2 \epsilon^2 + P_3 \epsilon^3 + \dots \quad (36)$$

in which coefficients are all constants dependent only on the parameter b . After $k - 1$ iterations, the network is renormalized to two end nodes, the Laplacian determinant is

$$\begin{aligned} \det [\mathbf{L}_k^{\mathbf{MK}} + \epsilon \mathbf{1}] &= C_k^{-2} b^{2k} \det \begin{bmatrix} q_k/2 & -p_k \\ -p_k & q_k/2 \end{bmatrix} \\ &= C_k^{-2} b^{2k} (q_k^2/4 - p_k^2), \end{aligned} \quad (37)$$

where the C_k^{-2} can be expressed in closed form,

$$\begin{aligned} C_k^{-2} &= (b^0 q_0)^{2^{k-1} b^k} (b^1 q_1)^{2^{k-2} b^{k-1}} (b^2 q_2)^{2^{k-3} b^{k-2}} \dots (b^{k-1} q_{k-1})^{2^{k-k} b} \\ &= \left(\prod_{\mu=0}^{k-1} b^{(2b)^{k-\mu} \mu/2} \right) \left(\prod_{\mu=0}^{k-1} q_\mu^b (2b)^{k-1-\mu} \right). \end{aligned}$$

The ansatz for fixed points of rescaled $\{q_\mu, p_\mu\}$ in Eq. (33) is

$$\begin{aligned} q_\mu &\sim 2^{-\mu} (Q_0 + \epsilon 4^\mu Q_1 + \epsilon^2 4^{2\mu} Q_2 \dots), \\ p_\mu &\sim 2^{-\mu} (Q_0/2 - \epsilon 4^\mu P_1/4 + \epsilon^2 4^{2\mu} P_2 + \dots). \end{aligned} \quad (38)$$

The fixed point scaling of parameters q_μ and p_μ in Eq. (38) verifies the validity of approximations in Eq. (33), since the differences between the approximated and exact parameters in Eq. (35) will not affect the scaling of any quantity we consider in Eq. (10). With respect to ϵ , we can calculate the j^{th} derivative of determinant for any b . Note that the asymptotic expression for $[C_k^{(k-1)}]^{-2}$ is approximated to

$$C_k^{-2} \sim \alpha^N \prod_{\mu=0}^{k-1} [q_\mu]^{b(2b)^{k-1-\mu}},$$

in which α is an ϵ -independent factor that remains irrelevant after the differentiation in Eq. (10).

The zeta-functions for the Laplacian determinants with varying b are eventually evaluated as

$$I_j \sim \begin{cases} N^{2j/(1+\log_2 b)-1} & 2j > (1 + \log_2 b) \\ \ln N & 2j = (1 + \log_2 b) \\ \text{const} & 2j < (1 + \log_2 b) \end{cases} \quad (39)$$

As we have argued in Ref. [17], we need to set

$$d_s = 1 + \log_2 b \quad (40)$$

to obtain the final result in Eq. (10).

-
- [1] L. K. Grover, Phys. Rev. Lett. **79**, 325 (1997).
 - [2] A. M. Childs and J. Goldstone, Phys. Rev. A **70**, 022314 (2004).
 - [3] S. Aaronson and A. Ambainis, *Proceedings of the 44th Annual IEEE Symposium on Foundations of Computer Science*, , 200 (2003).
 - [4] A. Ambainis, J. Kempe, and A. Rivosh, in *Proceedings of the sixteenth annual ACM-SIAM symposium on Discrete algorithms*, SODA '05 (Society for Industrial and Applied Mathematics, Philadelphia, PA, USA, 2005) pp. 1099–1108.
 - [5] A. M. Childs, Phys. Rev. Lett. **102**, 180501 (2009).
 - [6] E. Farhi and S. Gutmann, Phys. Rev. A **57**, 2403 (1998).
 - [7] A. M. Childs, E. Deotto, E. Farhi, J. Goldstone, S. Gutmann, and A. J. Landahl, Phys. Rev. A **66**, 032314 (2002).
 - [8] E. Farhi, J. Goldstone, S. Gutmann, and M. Sipser, arXiv preprint quant-ph/0001106 (2000).
 - [9] S. Chakraborty, L. Novo, A. Ambainis, and Y. Omar, Phys. Rev. Lett. **116**, 100501 (2016).
 - [10] R. Portugal, *Quantum Walks and Search Algorithms* (Springer, Berlin, 2013).
 - [11] A. M. Childs and J. Goldstone, Phys. Rev. A **70**, 042312 (2004).
 - [12] I. Foulger, S. Gnutzmann, and G. Tanner, Phys. Rev. Lett. **112**, 070504 (2014).
 - [13] A. M. Childs and Y. Ge, Phys. Rev. A **89**, 052337 (2014).
 - [14] S. Alexander and R. Orbach, J. Physique Lett. **43**, L625 (1982).
 - [15] R. Rammal, J. Physique **45**, 191 (1984).
 - [16] A. Bunde and S. Havlin, *Fractals in Science* (Springer-Verlag, 1994).
 - [17] S. Boettcher and S. Li, J. Phys. A (to appear, arXiv:1607.05168).
 - [18] E. Agliari, A. Blumen, and O. Milken, Phys. Rev. A **82**, 012305 (2010).
 - [19] S. Boettcher and S. Li, J. Phys. A **48**, 415001 (2015).
 - [20] P. Philipp, L. Tarrataca, and S. Boettcher, Phys. Rev. A **93**, 032305 (2016).
 - [21] A. Voros, *Advanced Studies in Pure Mathematics* **21**, 327 (1992).
 - [22] G. V. Dunne, J. Phys. A **45**, 374016 (2012).
 - [23] S. Boettcher, Euro. Phys. J. B **33**, 439 (2003).
 - [24] A. A. Migdal, J. Exp. Theo. Phys. **42**, 743 (1976).
 - [25] L. P. Kadanoff, Ann. Phys. **100**, 359 (1976).

- [26] A. N. Berker and S. Ostlund, *Journal of Physics C: Solid State Physics* **12**, 4961 (1979).
- [27] B. W. Southern and A. P. Young, *J. Phys. C: Solid State Phys.* **10**, 2179 (1977).
- [28] K. H. Fischer and J. A. Hertz, *Spin Glasses* (Cambridge University Press, Cambridge, 1991).
- [29] M. Plischke and B. Bergersen, *Equilibrium Statistical Physics, 2nd edition* (World Scientific, Singapore, 1994).
- [30] R. K. Pathria, *Statistical Mechanics, 2nd Ed.* (Butterworth-Heinemann, Boston, 1996).
- [31] P. Ramond, *Field Theory: A Modern Primer* (Westview Press, 1997).